ELSEVIER

Coordination Chemistry Reviews
190–192 (1999) 371–389

COORDINATION CHEMISTRY REVIEWS

www.elsevier.com/locate/ccr

Dinuclear metal complexes of bis-macrocycles

Thomas A. Kaden *

Institute of Inorganic Chemistry, Spitalstrasse 51, CH-4056 Basel, Switzerland

Accepted 13 March 1999

Contents

Abstract

Three bis-macrocycles **7**, **10**, **11**, consisting of two cyclononane units with a N_3, N_2S, and NS_2 donor set bridged by a pyrazole group, have been synthesized and their complexation potential studied. Several solid dinuclear compounds with Cu^{2+} and Ni^{2+} could be isolated and their structure elucidated. In all cases, the two metal ions are bound by the three donor atoms of the macrocycle, by the deprotonated pyrazole group and by one atom of the exogenous ligand, which bridges the two metal centres. In the case of the Cu^{2+} complexes, strong anti-ferromagnetic coupling was found. In solution, ligands **7** and **10** give a series of mononuclear $[Cu(LH_n)]$ ($n = 1, 0, -1$) and dinuclear $[Cu_2(LH_m)]$ ($m = 0, -1, -2, -3$) species which have been identified and characterized by potentiometric and spectrophotomet-

* Tel.: +41-61-2671006; fax: +41-61-2671020.
E-mail address: kaden@ubaclu.unibas.ch (T.A. Kaden)

PII: S0010-8545(99)00095-8

ric studies. Cyclic voltammetry and ES-MS have been used to study the ternary species in solution.

Keywords: Pyrazole group; Solid dinuclear compounds; Macrocycle

1. Introduction

The interest for dinuclear metal complexes stems from very different points of view [1]. On the one hand there is a theoretical interest for such compounds, since one can expect that two metal centres (especially if paramagnetic) kept at a fixed distance not too far from each other will interact. This is often reflected in their magnetic properties (EPR or magnetic moments) or in their electrochemistry. On the other hand dinuclear complexes are also interesting because two metal centres fixed at a certain distance often allow the binding and thus the recognition and/or activation of a substrate molecule. From this point of view, they can be used to mimic metalloproteins such as laccase [2], haemocyanin [3], superoxide dismutase [4], or urease [5] and to study structure/reactivity relationships [6].

Macrocycles have often been selected for this purpose because, being more rigid than open chain ligands, they allow one to fix the position and therefore the distance between the two metal ions in an easier way. Schematically, the different strategies are shown in Fig. 1.

The first type of such ligands (Fig. 1a) consists of a ring large enough to accommodate two metal ions in it [7]. Variations of the structures have produced systems in which the metal–metal distance can be controlled and thus different

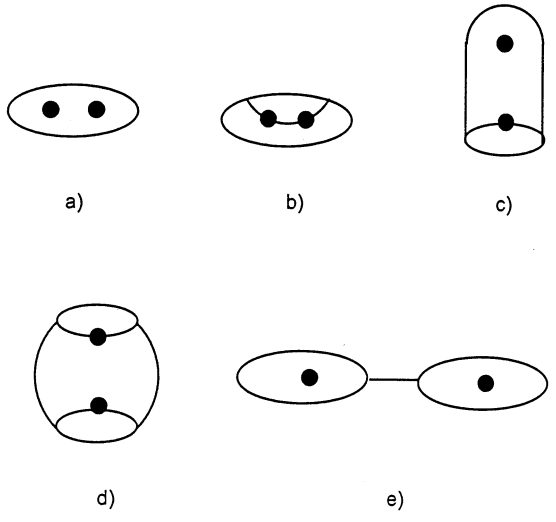

Fig. 1. Possible topologies for macrocyclic dinuclear complexes.

exogenous ligands can be bound. The idea of large rings has also been developed into macrobicyclic systems with axial (Fig. 1b), lateral (Fig. 1c), and cylindrical (Fig. 1d) topologies [8]. Again, by variation of the donor sets and the length of the linking groups, the two metal ions can be fixed at a desired distance from each other.

A different approach is found in the case of bis-macrocycles (Fig. 1e) in which two rings are connected either by a carbon–carbon [9] or a nitrogen–nitrogen [10] linker. Depending on its length the metal–metal interaction can be controlled and thus tuned. Most of the bis-macrocycles are homotopic, i.e. have two identical rings with the same donor sets. However, heteroditopic bis-macrocycles have also been prepared [11], although their synthesis is more demanding than that of homoditopic systems. Heteroditopic ligands of course offer the possibility to prepare heterodinuclear complexes in an easier way.

A further class of bis-macrocycles are compounds which have additional donor groups in the bridging unit. Examples with alcoholate [12] or pyrazolide [13,14] bridging moieties show that the donor group of the chain connecting the two rings also can coordinate. We have studied in detail one of these systems and the syntheses of the ligands, their dinuclear complexes and the properties of them will be reported below.

2. Synthesis of the pyrazole bridged bis-macrocycles

The syntheses of the three ligands **7**, **10** and **11** were carried out by *N*-alkylations of the corresponding macrocycles **1**, **3** and **8** with 3,5-bis(chloromethyl)-1*H*-pyrazole hydrochloride (**4**) as bifunctional alkylating agent (Scheme 1) [14].

For the preparation of **7** and **10** the selective protection of the macrocycle is necessary, to ensure that only mono-alkylation takes place. In both cases *N*,*N*-dimethylformamide dimethylacetal was used as a protecting group [15] [16]. For the synthesis of **7**, 3,5-bis(chloromethyl)-1*H*-pyrazole (**4**) reacted with the tricyclic orthoamide **1** to give the salt **5**, which precipitates from the solution in high purity. This compound was then hydrolysed first to the diformyl substituted product **6** and then to **7**. The new synthesis of **7** is easier and gives better yields than the one previously described [13]. Compound **10** was synthesized by reacting the corresponding monoformyl protected macrocycle **8**, which was obtained through controlled hydrolysis of the cyclic aminal [16]. For 1-aza-4,7-dithiacyclononane (**3**) of course no protection at all is needed. The cleavage of the formyl groups of **6** and **9** was carried out under acid and basic conditions, respectively.

All three ligands, identified and characterized by analytical and spectroscopical methods, give dinuclear Cu^{2+} (**12**, **13a**, **13b**, **13c**, **14a**, **14b**, **14c**) and Ni^{2+} (**15**) complexes (Scheme 1).

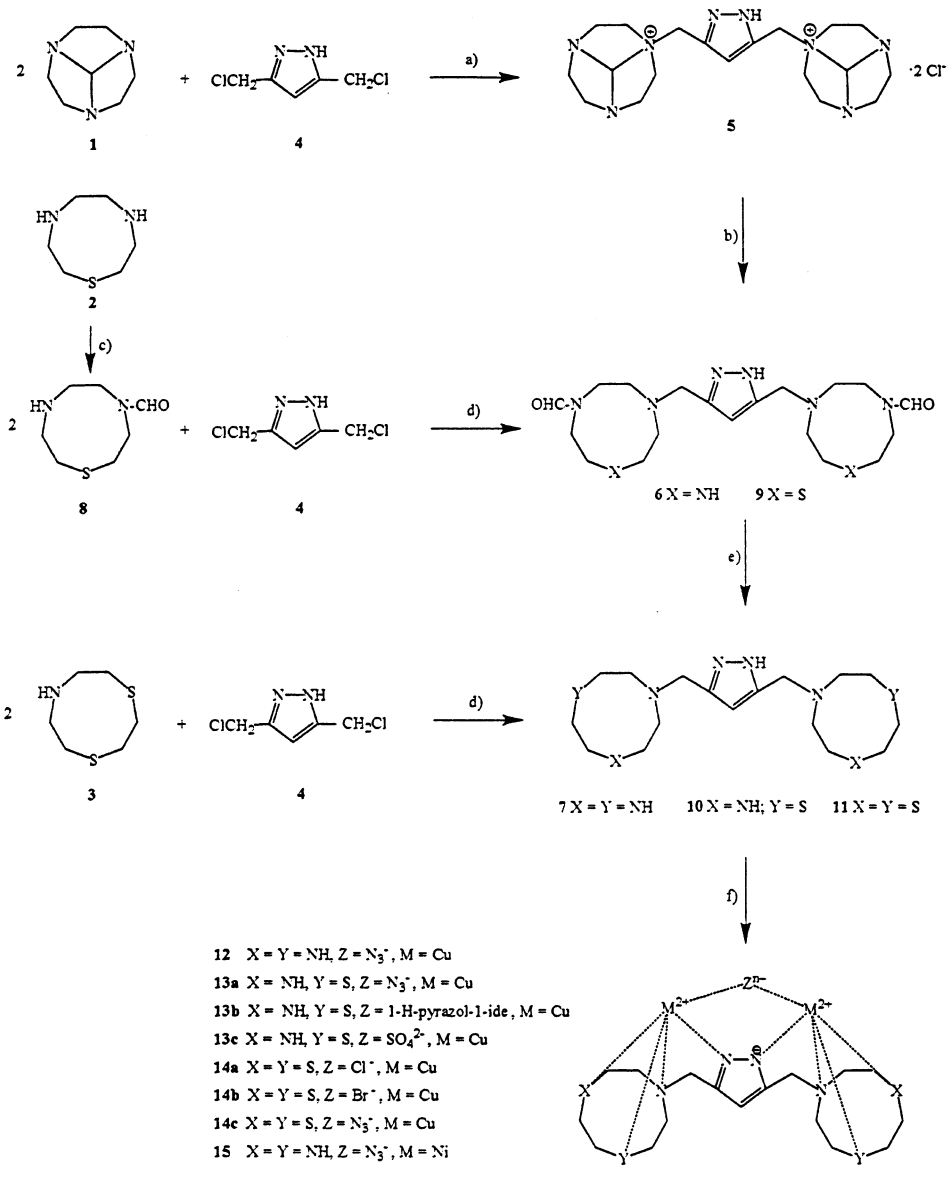

a) 1 equ. NEt_3, CH_3CN, 80°, 2 h ; b) H_2O, 100°, 24 h ; c) 1) N,N-dimethylformamide dimethylacetal, benzene, 80°, 30 min., 2) EtOH / H_2O ; d) Na_2CO_3, CH_3CN, 80°, 28 h ; e) 10 % NaOH, 100°, 5h (**10**), or 3 N HCl, 70°, 2 h (**7**) ; f) 2 M^{2+}, Z^{n-}

Scheme 1.

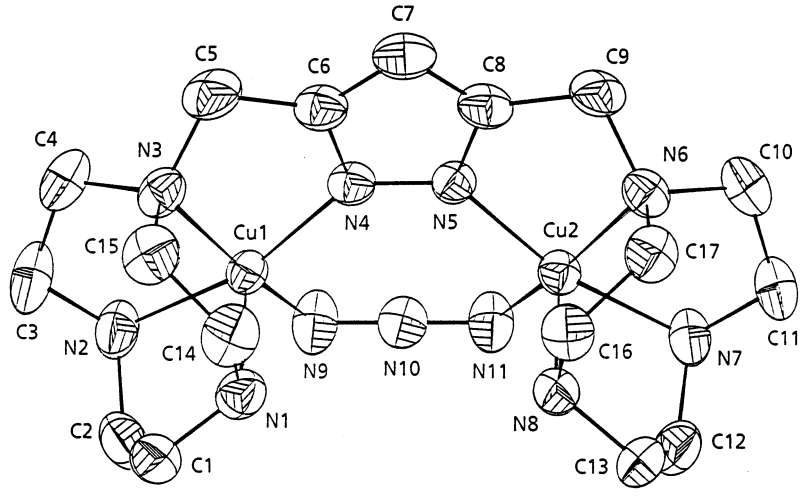

Fig. 2. ORTEP plot of **12**.

3. Properties of the dinuclear complexes as solids

3.1. X-ray structures

The X-ray structures of the dinuclear Cu^{2+} complexes **12**, **13c**, **14a**, and **14b** are shown in Figs. 2–5.

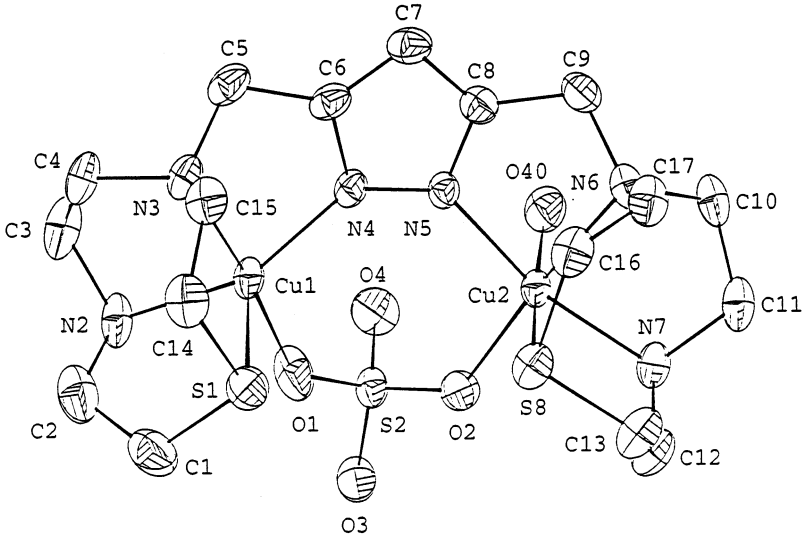

Fig. 3. ORTEP plot of **13c**.

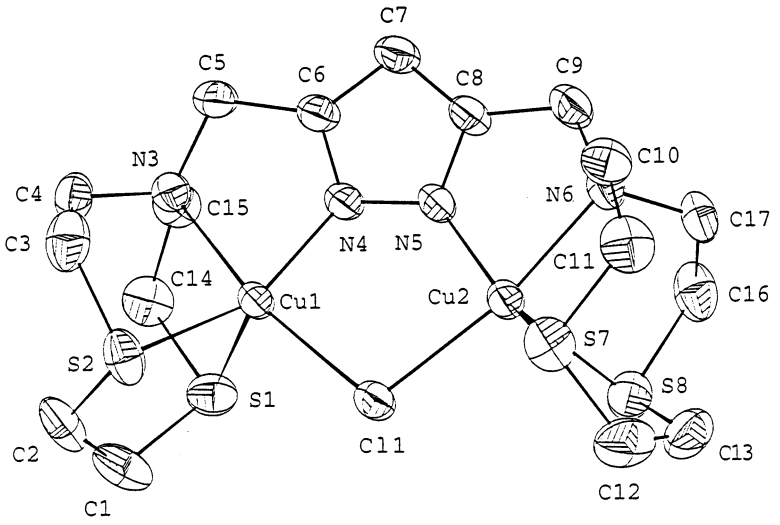

Fig. 4. ORTEP plot of **14a**.

In all these structures exogenous bridging ligands are present. Each Cu^{2+} is coordinated by the three donor atoms of the macrocycle, one pyrazolodiyl nitrogen and one atom of the exogenous bridging ligand. Remarkably, in the dinuclear Cu^{2+} complex **13c** one finds two different coordination geometries with different coordination numbers (Fig. 3). The coordination geometry of Cu(1) is distorted trigonal bipyramidal with N(3) and O(1) of the sulfato group in the axial positions. In contrast, Cu(2) exhibits a distorted octahedral coordination with an additional

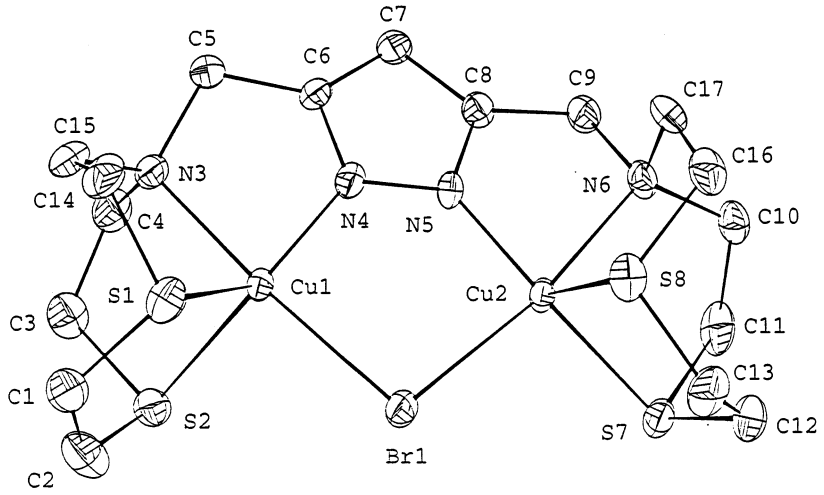

Fig. 5. ORTEP plot of **14b**.

Table 1
Selected bond lengths [Å] of **12**, **13c**, **14a**, and **14b**

	12	**13c**	**14a**	**14b**
Cu(1)–Cu(2)	4.150(1)	4.156(1)	3.697(1)	3.760(1)
Cu(1)–X(1) [a]	2.000(4)	1.947(4)	2.373(1)	2.482(1)
Cu(1)–N(1)	2.164(4)			
Cu(1)–S(1)		2.529(1)	2.465(1)	2.429(2)
Cu(1)–N(2)	1.994(4)	2.007(4)		
Cu(1)–S(2)			2.334(1)	2.350(2)
Cu(1)–N(3)	2.061(3)	2.076(4)	2.128(2)	2.120(6)
Cu(1)–N(4)	1.938(3)	1.926(4)	1.886(2)	1.875(6)
Cu(2)–X(2) [a]	1.987(4)	1.987(3)	2.359(1)	2.488(1)
Cu(2)–N(8)	2.180(4)			
Cu(2)–S(8)		2.596(1)	2.438(1)	2.492(2)
Cu(2)–N(7)	1.990(4)	2.019(4)		
Cu(2)–S(7)			2.351(1)	2.302(2)
Cu(2)–N(6)	2.070(3)	2.071(4)	2.135(2)	2.107(6)
Cu(2)–N(5)	1.934(3)	1.951(3)	1.877(2)	1.885(6)
Cu(2)–O(40)		2.600(4)		

[a] X(1) and X(2) are the atoms of the bridging group. For **12**, N(9) and N(11) of the N_3^-; for **13c**, O(1) and O(2) of the SO_4^{2-}; for **14a**, Cl(1); and for **14b**, Br(1).

oxygen (O(40)) of a water molecule in the sixth position. The deviations from the best plane through N(5), N(6), N(7) and O(2) are ± 0.02 Å, the central ion being located 0.05 Å out of this plane. The bond lengths between the Cu^{2+} centres and the pyrazolide nitrogens are slightly shorter (ca. 0.1 Å) than normal Cu–N bond lengths, due to negative charge on the pyrazole moiety. The Cu(1)–Cu(2) distance is 4.16 Å (Table 1).

The structures of **14a** and **14b** are very similar to each other (Figs. 4 and 5). They show distorted trigonal bipyramidal coordination geometries around each copper ion. One axial position of each trigonal bipyramid is occupied by the bridging halogenide ion, the other one by the nitrogens N(3) and N(6), respectively. In these complexes too, the negative charge of the pyrazolide nitrogens results in slightly shorter Cu–N–bonds (Table 1). The Cu(1)–Cu(2) distances in the two halogenide bridged complexes are almost identical (3.70 Å for **14a** and 3.76 Å for **14b**).

The structures of the two azide bridged dinuclear Cu^{2+} and Ni^{2+} complexes are quite different.

The Cu^{2+} complex **12** strongly resembles the ones just discussed, each Cu^{2+} being pentacoordinate in a somewhat distorted square pyramidal geometry (Fig. 2). Here one finds three different Cu–N-bond lengths: the shortest one is that to the deprotonated pyrazole, then normal bond lengths to two amino nitrogens of the macrocycle, and finally a rather long one to the third nitrogen atom of the ring (Table 1). The two Cu^{2+} ions, the azide and the pyrazolide N-atoms form a nearly planar arrangement. The Cu^{2+}–Cu^{2+} distance is 4.15 Å (Table 1).

In contrast, the structure of the dinuclear Ni^{2+} complex **15** shows two hexacoordinate metal centres (Fig. 6). The three donors of the 1,4,7-triazacyclononane

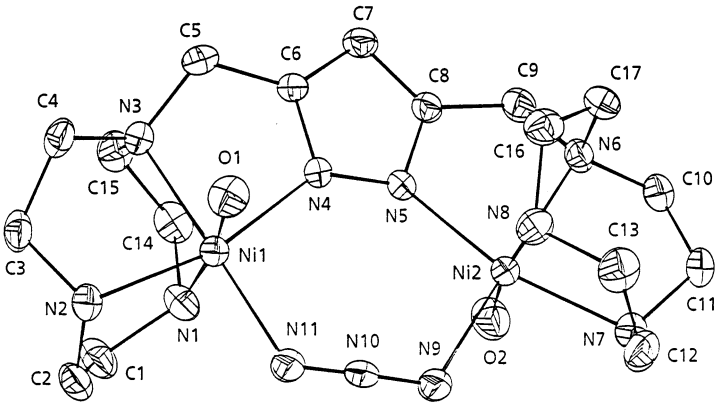

Fig. 6. ORTEP plot of **15**.

moiety, a nitrogen from the pyrazolide and one of the bridging azide, as well as a water molecule coordinate to each metal ion to give a distorted octahedral geometry. Interestingly, in contrast to the structures of the Cu^{2+} complexes discussed above, the arrangement of the two facially coordinated macrocycles, and therefore of the two water molecules also, is *transoid*. The Ni–N bonds are in their normal range and the Ni(1)–Ni(2) distance is 4.45 Å (Table 2).

3.2. Magnetic properties

The magnetic moments of the dinuclear Cu^{2+} complexes **12**, **13a**, **13b**, and **14a** at room temperature are distinctly lower than expected for two independent paramagnetic Cu^{2+} ions, which is indicative for an antiferromagnetic coupling. The temperature dependence of the corrected magnetic susceptibility was analyzed with the *Bleaney–Bowers* equation (Eq. (1)) [17],

$$\chi_{\mathrm{mol}} = \frac{N\beta^2 g^2}{3kT}\cdot\left(1+\frac{1}{3}\,\mathrm{e}^{\frac{-2J}{kT}}\right)^{-1}\cdot(1-\rho)+\frac{N\beta^2 g^2}{4kT}\cdot\rho+N_\alpha \qquad (1)$$

Table 2
Selected bond lengths in **15**

Å		Å	
Ni(1)–Ni(2)	4.450(1)		
Ni(1)–O(1)	2.161(3)	Ni(2)–O(2)	2.167(3)
Ni(1)–N(1)	2.093(3)	Ni(2)–N(6)	2.121(3)
Ni(1)–N(2)	2.097(3)	Ni(2)–N(7)	2.086(4)
Ni(1)–N(3)	2.115(3)	Ni(2)–N(8)	2.074(4)
Ni(1)–N(4)	2.041(3)	Ni(2)–N(5)	2.041(3)
Ni(1)–N(11)	2.102(4)	Ni(2)–N(9)	2.106(4)

Table 3
Magnetic parameters obtained from the temperature dependence of χ_{mol} for **12**, **13a**, **13b** and **14a**

Complex	g	$-2J$ (cm^{-1})	N_α (10^6 cm^3 mol^{-1})	ρ	μ_{eff} (BM) at 300 K
12	2.07 [a]	>1000	80	2.8×10^{-2}	0.65
13a	2.1 [a]	>1000	51	5.9×10^{-3}	0.47
13b	2.1 [a]	300	37	–	1.42
14a	2.0 [a]	272	52	2.3×10^{-2}	1.37

[a] Kept fixed during the fitting procedure.

using the isotropic exchange Hamiltonian ($H=-2JS_1S_2$) for two interacting centres with $S=1/2$. The corrected molar susceptibility χ_{mol} is expressed per mole of copper atom, N_α is the temperature independent paramagnetism, and ρ, the fraction of paramagnetic impurity. The other symbols have their usual meaning.

The experimental data were least-squares fitted to the theoretical expression, keeping the value of g fixed and all other parameters variable (Table 3). The spin–spin interaction within the complex is highly dependent on the nature of the exogenous ligand. The azide bridged complexes **12** and **13a** exhibit a low magnetic susceptibility over a wide temperature range. Both the high $-2J$ values (>1000 cm^{-1}) and the low magnetic moments at room temperature of 0.65 BM and 0.47 BM for **12** and **13a**, respectively, indicate a very strong antiferromagnetic coupling. This results from the fact that the HOMOs of the pyrazolide and azide, both of which are bridging the Cu^{2+} ions, are antisymmetric so that both of them interact with the antisymmetric combination of the $d_{x^2-y^2}$ orbitals of the Cu^{2+} ions, stabilizing, very strongly, the singlet state [18]. The temperature dependencies of χ_{mol} for **13b** and **14a** allow the determination of the values $-2J=300$ cm^{-1} for **13b** and $-2J=272$ cm^{-1} for **14a**. The two complexes behave similarly and demonstrate antiferromagnetic coupling only at low temperatures, whereas at 300 K the magnetic moments are 1.42 and 1.37 BM, respectively.

4. Studies of the dinuclear complexes in solution

4.1. Electrochemistry

The cyclic voltammetry of the dinuclear Cu^{2+} complexes is characterized by two one electron processes due to two reduction and two oxidation steps, respectively (Fig. 7). They describe the redox transitions $Cu(II)/Cu(II)\rightarrow Cu(II)/Cu(I)$ (a) and $Cu(II)/Cu(I)\rightarrow Cu(I)/Cu(I)$ (b) in both directions.

The differences between $E_{1/2}$ (a) and $E_{1/2}$ (b), (220 and 252 mV), are clearly larger than the statistical value of 35.6 mV expected for two independent Cu^{2+} centres [19]. Comparing the redox potentials of the different complexes, a strong dependence on the nature of the donor atoms of the bis-macrocycle as well as on the type of bridging ligand can be observed (Table 4).

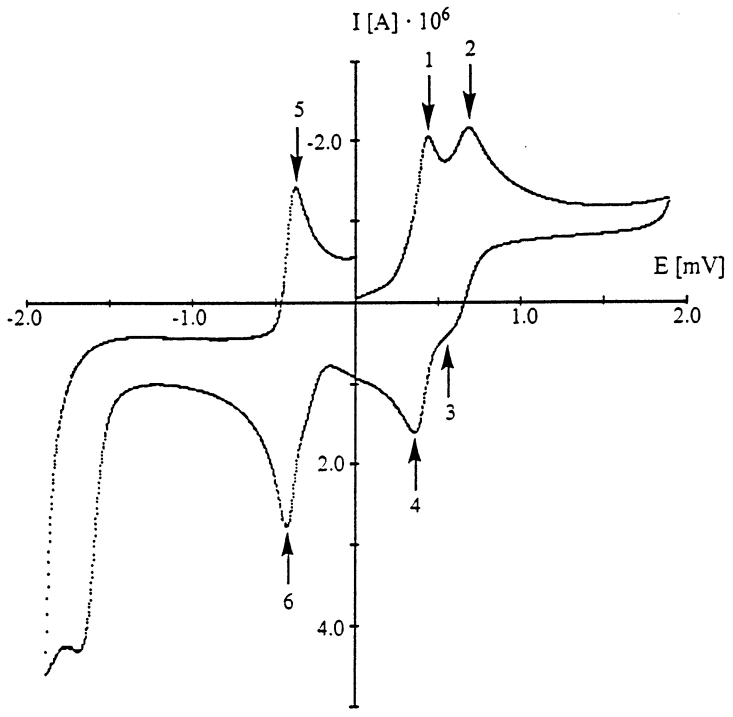

Fig. 7. Cyclic voltammetry of **13b** in acetonitrile (Peaks 5 and 6 ferrocenium/ferrocene couple).

In the series of the bis-macrocycles **7**, **10** and **11**, the number of sulfur donors steadily increases, whereas the number of nitrogens decreases. This makes the ligand softer and more prone to stabilize the Cu(I) over the Cu(II) oxidation state. In the azide bridged complexes **12**, **13a**, and **14**, the potential is shifted by more than 500 mV to more positive values. In addition the potentials are also determined by the nature of the bridging ligand. The dinuclear Cu^{2+} complex of **10** with azide as a bridging group (**13a**) has a more positive potential than that with pyrazolide (**13b**).

Table 4
Half-wave potentials (in mV) versus NHE from the CV of the dinuclear Cu^{2+} complexes **12**, **13a**, **13b** and **14**

Complex	Ligand	Z	$E_{1/2}$ (a)	$E_{1/2}$ (b)	ΔE (a)	ΔE (b)
12	**7**	Azide	−329	−549	150	90
13a	**10**	Azide	−200	−449	63	72
14	**11**	Azide	+211	−41	63	125
13b	**10**	Pyrazolide	−402	−635	85	132

Table 5
Protonation constants of **7** and **10** and of their Cu^{2+} complexes (at 25°C and $I = 0.5$ M (KNO_3)) as well as spectral properties (λ_{max} and ε) of the Cu^{2+} complexes

	7		**10**	
Species	pK_H [a]	λ_{max} (ε) [b]	pK_H [a]	λ_{max} (ε) [b]
LH_4^{4+}	6.08(1)	–		
LH_3^{3+}	6.80(1)	–	2.19 (1)	–
LH_2^{2+}	10.54(2)	–	10.05 (1)	–
LH^{+}	11.25(2)	–	10.72 (2)	–
$[Cu(LH_2)]^{4+}$	5.90(2)	650(115)		
$[Cu(LH)]^{3+}$	7.08(2)	644(120)	6.33 (4)	637 (116)
$[Cu(L)]^{2+}$	10.70(1)	624(110)	10.12 (4)	612 (114)
$[Cu(LH_{-1})]^{+}$	–	[c]	10.76 (2)	602 (123)
$[Cu(LH_{-2})]$	–	–	–	[c]
$[Cu_2(L)]^{4+}$	3.69(2)	649(179)	2.41 (1)	[c]
$[Cu_2(LH_{-1})]^{3+}$	6.85(1)	647(238)	6.59 (1)	627 (232)
$[Cu_2(LH_{-2})]^{2+}$	–	626(233)	11.71 (1)	612 (221)
$[Cu_2(LH_{-3})]^{+}$	–	–	–	[c]

[a] Mean value and standard deviation between four batches.
[b] λ_{max} in nm and ε in $M^{-1}\ cm^{-1}$.
[c] Cannot be determined.

4.2. Speciation and stability constants [13] [20]

The fitting of the potentiometric titrations of **7** and **10** in the presence of 0.9 or 1.8 equivalents of Cu^{2+} allow in a batch calculation, in which the experimental points of both titration curves are used at the same time to calculate the stability of the mononuclear species $[Cu(LH)]^{3+}$, $[Cu(L)]^{2+}$, $[Cu(LH_{-1})]^{+}$ and $[Cu(LH_{-2})]$ as well as of the dinuclear complexes $[Cu_2(L)]^{4+}$, $[Cu_2(LH_{-1})]^{3+}$, $[Cu_2(LH)_{-2})]^{2+}$, and $[Cu_2(LH)_{-3})]^{+}$. Since the absolute stability of these species could not be determined by potentiometry, $[Cu(LH)]^{3+}$ being already fully formed at low pH, we describe the system with pK_H values (Eq. (2)) connecting the protonated species and their conjugate bases (Table 5). In the case of **7**, however, the stability of $[Cu(LH)]^{3+}$ was measured by spectrophotometric titrations so that the absolute values are known here [13].

$$Cu(LH_n) \rightleftharpoons Cu(LH_{n-1}) + H^{+};\ K_n = ([Cu(LH_{n-1})]\cdot[H^{+}])/[Cu(LH_n)] \qquad (2)$$

Since both ligands give very similar species we shall discuss as an example only those formed by **10**. The species distribution for **10** with $[L] = 2.5 \times 10^{-3}$ M and $[Cu^{2+}] = 2.3 \times 10^{-3}$ M show (Fig. 8) that $[(CuLH)]^{3+}$ dominates at a pH below 6, whereas the main species between pH 6 and 11 are $[CuL]^{2+}$ and $[Cu(LH_{-1})]^{+}$. $[Cu(LH_{-2})]$ exists in measurable concentrations only above pH 11.

In $[Cu(LH)]^{3+}$ (**16**) the Cu^{2+} ion is coordinated by one of the N_2S-rings, whereas the proton is located on a nitrogen of the second ring not involved in coordination of the metal ion (Scheme 2).

The three deprotonation steps of $[Cu(LH)]^{3+}$ to give $[CuL]^{2+}$, $[Cu(LH_{-1})]^{+}$, and $[Cu(LH_{-2})]$ involve the neutralization and concomitant coordination of the pyrazole group, the formation of a hydroxo species and the deprotonation of the ammonium group of the N_2S ring. Whereas the structure of the final product (**19**) is clear, the exact sequence of the deprotonations is more difficult to determine. The shift of the absorption maximum from 637 nm for $[Cu(LH)]^{3+}$ to 612 nm for $[CuL]^{2+}$ (Table 5) indicates that it is in this step that the formation and coordination of the pyrazolide group takes place, whereby the ligand field increases. So the structure of $[CuL]^{2+}$ must be **17**. The exact sequence of the other two deprotonation steps is even more difficult to determine since they occur very close to each other (structures **18** and **19**, Scheme 2).

Ligand **10** was specifically designed to form dinuclear complexes and indeed in aqueous solution we find such species, which differ in their protonation degree. For example for L = **10** in a mixture with $[L] = 2.5 \times 10^{-3}$ M and $[Cu^{2+}] = 4.6 \times 10^{-3}$ M, $[Cu_2L]^{4+}$ is formed already at very low pH and deprotonates with $pK_H = 2.41$ to give $[Cu_2(LH_{-1})]^{3+}$ (Fig. 9). The structure of $[Cu_2L]^{4+}$ (**20**) can thus be described by two Cu^{2+} symmetrically coordinated by the two macrocyclic rings, whereas that of $[Cu_2(LH_{-1})]^{3+}$ (**21**) with a maximum at 627 nm has in addition the pyrazolide bridging group coordinated at each Cu^{2+}, as was found in the solid state structures (see above). Further deprotonation to $[Cu_2(LH_{-2})]^{2+}$ (**22**) and $[Cu_2(LH_{-3})]^{+}$ (**23**) gives the mono- and dihydroxo moieties (Scheme 2).

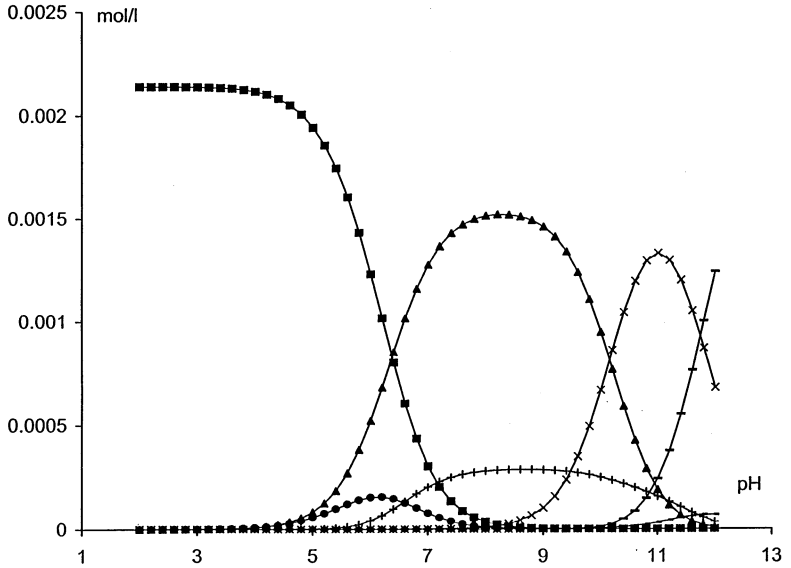

Fig. 8. Species distribution of the complexes of **10** with 0.9 equivalents Cu^{2+}. $[L] = 2.5 \times 10^{-3}$ M, $[Cu^{2+}] = 2.3 \times 10^{-3}$ M. ■, $[Cu(LH)]^{3+}$; ▲, $[CuL]^{2+}$; **X**, $[Cu(LH_{-1})]^{+}$; –, $[Cu(LH_{-2})]$; ●, $[Cu_2(LH_{-1})]^{3+}$; +, $[Cu_2(LH_{-2})]^{2+}$.

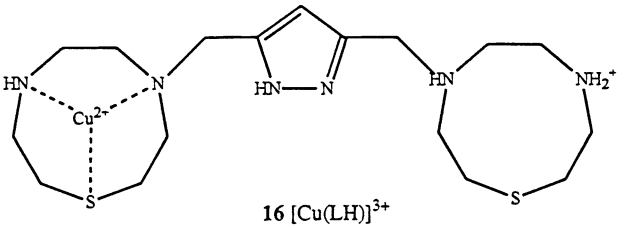

16 $[Cu(LH)]^{3+}$

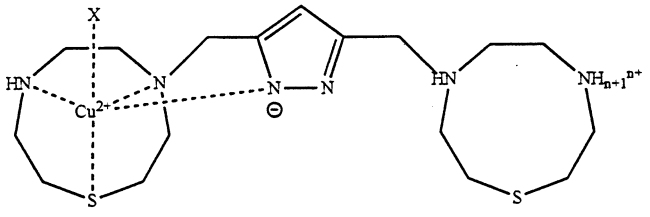

17 $[Cu(L)]^{2+}$ $X = H_2O$, n = 1

18 $[Cu(LH_{-1})]^{+}$ $X = OH^-$, n = 1 or $X = H_2O$, n = 0

19 $[Cu(LH_{-2})]$ $X = OH^-$, n = 0

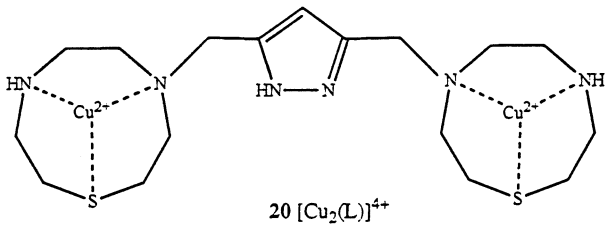

20 $[Cu_2(L)]^{4+}$

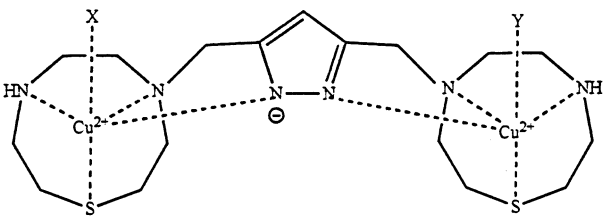

21 $[Cu_2(LH_{-1})]^{3+}$ $X = Y = H_2O$

22 $[Cu_2(LH_{-2})]^{2+}$ $X = OH^-$; $Y = H_2O$

23 $[Cu_2(LH_{-3})]^{+}$ $X = Y = OH^-$

Scheme 2.

4.3. Ternary species

Since the *X-ray* studies showed that the dinuclear complex $[Cu_2(LH_{-1})]^{3+}$ is able to bind exogenous bridging ligands, it was interesting to study this reaction in solution. By spectrophotometric titrations, one can follow the formation of the ternary species as indicated in Eqs. (3) and (4).

$$[Cu_2(LH_{-1})]^{3+} + Z \rightleftharpoons [Cu_2(LH_{-1})Z];\ K_1 \tag{3}$$

$$2[Cu_2(LH_{-1})]^{3+} + Z \rightleftharpoons [[Cu_2(LH_{-1})]_2Z];\ K_2 \tag{4}$$

As bridging ligands N_3^-, pyrazole (pyr), and 1H,1′H-4,4′-methanediyl-bispyrazole (bispyr) were studied [20]. The results (conditional stabilities at pH 5.5) obtained by fitting the titration with the program SPECFIT [21] are interesting since they show that N_3^- and bispyr can form 1:1 and 2:1 species, whereas pyr as expected, only gives a 1:1 complex (Table 6).

To confirm these findings we have studied the system with bispyr also by electrospray mass spectrometry (ES-MS). By mixing $[Cu_2(LH_{-1})]^{3+}$ and bispyr in different ratio in the presence of a base one can see how the ternary species $[Cu_2(LH_{-1})]$bispyr] and $[[Cu_2(LH_{-1})]_2$bispyr] are indeed formed (Fig. 10).

The ES-MS of the complex without bispyr (ratio 1:0) shows the presence of several doubly charged ions (m/z 264.1, 277.1), which may correspond to solvent cluster ions of the complex $[Cu_2(LH_{-1})]^{3+}$. A small addition of bispyr results in the

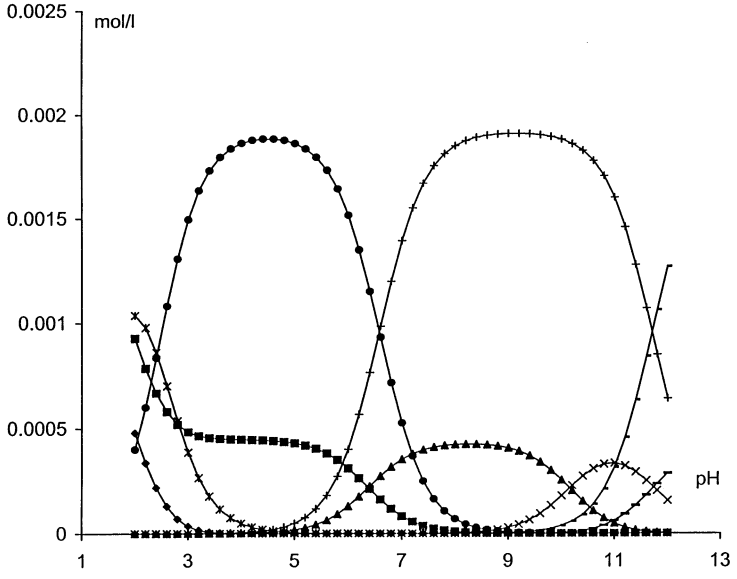

Fig. 9. Species distribution of the complexes of 10 with 1.8 equivalents Cu^{2+}. $[L] = 2.5 \times 10^{-3}$ M, $[Cu^{2+}] = 4.5 \times 10^{-3}$ M. ◆, Cu^{2+}; ■, $[Cu(LH)]^{3+}$; ▲, $[CuL]^{2+}$; **X**, $[CuLH_{-1})]^{+}$; –, $[Cu(LH_{-2})]$; ✱, $[Cu_2(L)]^{4+}$; ●, $[Cu_2(LH_{-1})]^{3+}$; +, $[Cu_2(LH_{-2})]^{2+}$.

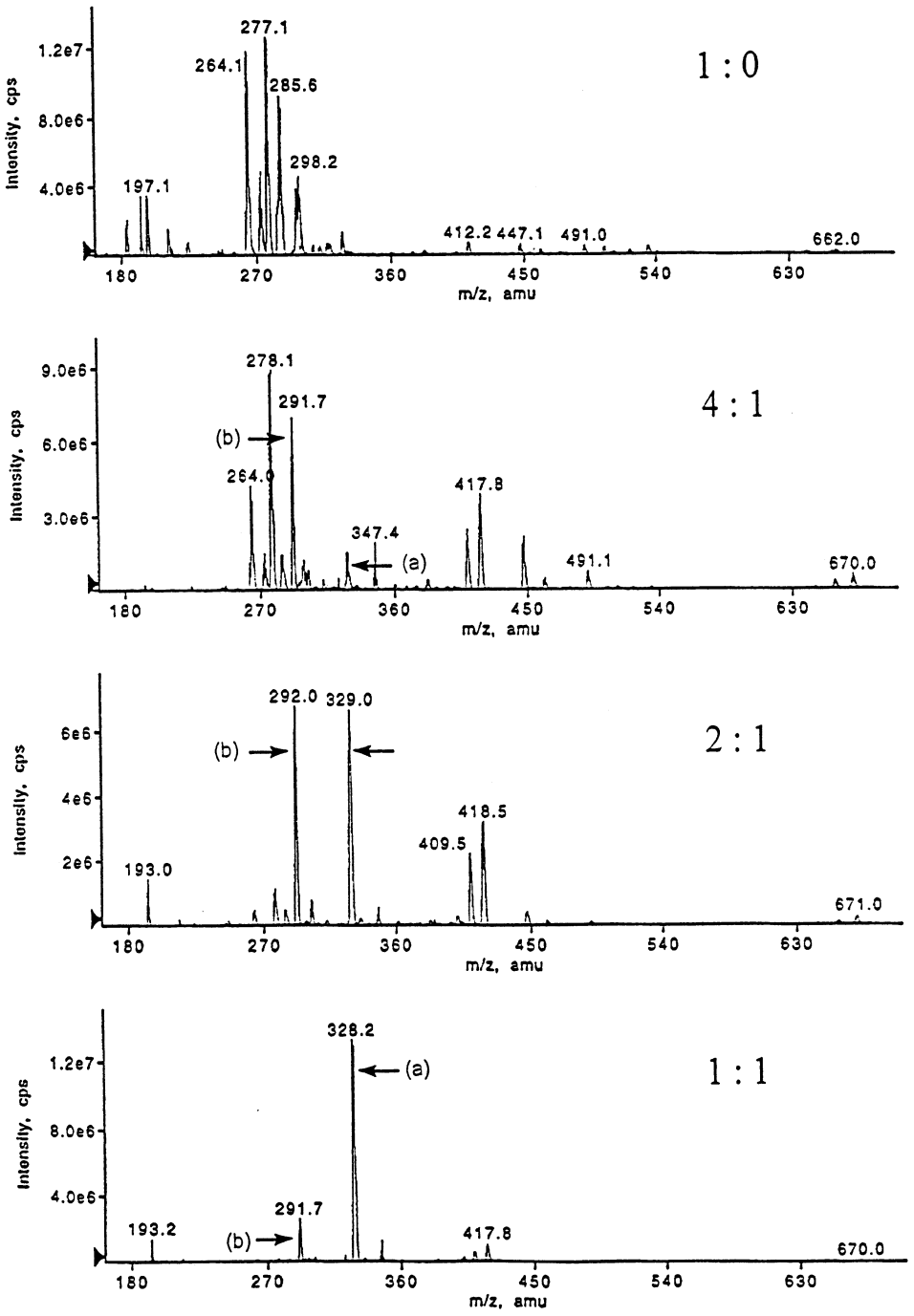

Fig. 10. ES-MS of the complex $[Cu_2(LH_{-1})]^{3+}$ (L = **10**) in presence of different amounts of bispyr, showing the formation of $[(Cu_2(LH_{-1})]_2$bispyr$]^{4+}$ (a) and $[Cu_2(LH_{-1})$bispyr$]^{2+}$ (b).

Table 6
Conditional stability constants (pH 5.5) for the formation of the ternary complexes of $[Cu_2(LH_{-1})]$ (L = **10**) with N_3^-, pyr and bispyr according to Eqs. (3) and (4) at 25°C and $I = 0.5$ M KNO_3

	N_3^-	Pyr	Bispyr
log K_1	4.22(5)	3.85(3)	3.85 [a]
log K_2	7.27(6)	–	7.65(5)

[a] Kept fixed during the fitting procedure.

appearance of the ions at m/z 292.2 and 329.0 corresponding to a quadruplly and doubly charged species, which become predominant at a ratio of 2:1. The isotopic distribution of the ion at m/z 292.2 is in good agreement with a complex corresponding to $[[Cu_2(LH_{-1})]_2bispyr]^{4+}$, while the ion at m/z 329.0 fits with the complex $[Cu_2(LH_{-1})bispyr]^{2+}$. Electrospray ionization mass spectrometry reflects generally qualitatively the species present in solution [22]. Since intensities of the ions observed in the spectra are strongly charge and compound dependent, the signal intensities can not be used quantitatively. However, at a 1:1 ratio $[Cu_2(LH_{-1})bispyr]^{2+}$ is almost exclusively observed. For the structures of these two complexes we propose **24** and **25** (Scheme 3).

Species **25** is an interesting moiety which self-assembles from seven species by mixing four equivalents of Cu^{2+}, two equivalents of ligand **10**, one equivalent of bispyr, and enough base to deprotonate the pyrazole rings.

5. Conclusions

In conclusion we can say that the three ligands **7**, **10**, and **11**, consisting of two macrocyclic units with a N_3, N_2S, or NS_2-donor set bridged by a pyrazole unit are able to give a variety of metal complexes. Whereas in solution, a series of mononuclear $[Cu(LH_n)]$ ($n = 1, 0, -1$) and dinuclear $[Cu_2(LH_m)]$ ($m = 0, -1, -2, -3$) species have been identified, only dinuclear complexes were isolated as solids.

The structures and properties of the dinuclear species have been studied. In all cases the metal ion is coordinated by the three donor atoms of the macrocycle, by the deprotonated pyrazole and by an additional exogenous bridging ligand. The metal–metal distance depends on the external ligand and shows that the complex is flexible enough to adapt itself to the electronic and steric requirements of the exogenous ligand. In the case of the Cu^{2+} complexes strong antiferromagnetic coupling between the two metal centres has been observed, especially when N_3^- is the exogenous ligand. In addition cyclic voltammetry indicates that the two Cu(II) can be reduced in two steps to Cu(I).

In solution, the dinuclear complexes are also able to bind exogenous ligands, such as N_3^-, pyr and bispyr, which bridge the two metal ions. In one case ES-MS has been used to prove the existence of such ternary species in solution.

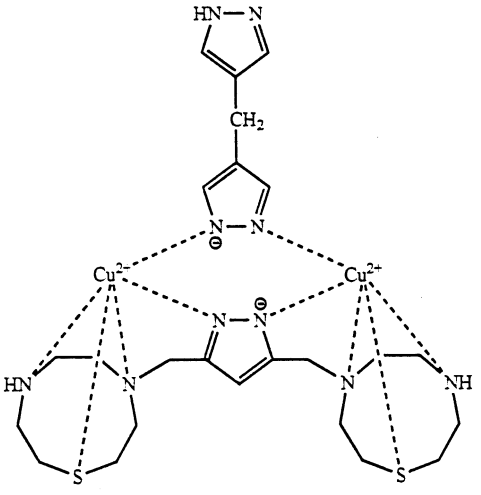

24 $[Cu_2(LH_{-1})bispyr]^{2+}$

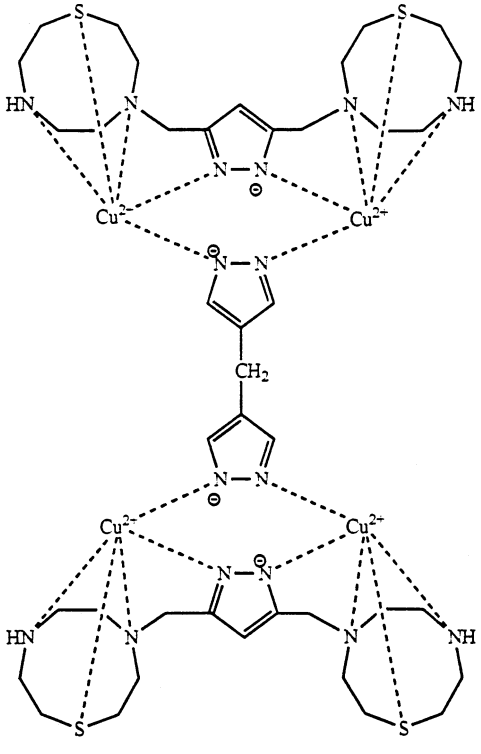

25 $[[Cu_2(LH_{-1})]_2bispyr]^{4+}$

Scheme 3.

Acknowledgements

This work was supported by the Swiss National Science Foundation (Project N. 2000-52225.97) and this is gratefully acknowledged.

References

[1] (a) E. Bouwman, W.L. Driessen, J. Reedijk, Coord. Chem. Rev. 104 (1990) 143. (b) N. Kitajima, Y. Morooka, Chem. Rev. 94 (1994) 737. (c) E.I. Solomon, M.J. Baldwin, M.D. Lowery, Chem. Rev. 92 (1992) 521. (d) E. Spodine, J. Manzur, Coord. Chem. Rev. 119 (1992) 171. (e) Th. A. Kaden, in: L. Fabbrizzi, A. Poggi (Eds.), Transition Metals in Supramolecular Chemistry, Kluwer Academic, 1994, pp. 211.

[2] J.L. Cole, P.A. Clark, E.J. Solomon, J. Am. Chem. Soc. 116 (1994) 7682.

[3] (a) K.A. Magnus, H. Ton-That, J.E. Carpenter, Chem. Rev. 94 (1994) 727. (b) J. Ling, L.P. Nestor, R.S. Czernuszewicz, T.G. Spiro, R. Fraczkiewicz, K.D. Sharma, T.M. Loehr, J. Sanders-Loehr, J. Am. Chem. Soc. 112 (1990) 9548.

[4] (a) J.A. Tainer, E.D. Getzoff, J.S. Richardson, D.C. Richardson, Nature (London) 306 (1983) 284. (b) A. Gärtner, U. Weser, Top. Curr. Chem. 132 (1986) 1. (c) E.G. Cass in: Metalloproteins, part 1, VCH Publishers, Weinheim, 1985, pp.121. (d) I. Fridovitch, J. Biol. Chem. 264 (1989) 7761.

[5] D.A. Clark, D.E. Wibon, Inorg. Chem. 28 (1989) 1326.

[6] (a) K. Karlin, J. Zubieta (Eds.), Copper Coordination Chemistry: Biochemical and Inorganic Perspectives, Academic Press, New York 1983. (b) K. Karlin, J. Zubieta (Eds.), Biological and Inorganic Copper Chemistry, vols. I and II, Academic Press, New York, 1986.

[7] (a) R.W. Stotz, R.C. Stoufer, J. Chem. Soc. Chem. Commun. (1970) 1682. (b) M. Micheloni, P. Paoletti, A. Bianchi, Inorg. Chem. 24 (1985) 3702. (c) A. Bencini, A. Bianchi, E. Garcia-España, S. Mangani, M. Micheloni, P. Orioli, P. Paoletti, Inorg. Chem. 27 (1988) 1104. (d) M. Yamashita, H. Ito, T. Ito, Inorg. Chem. 22 (1983) 2101. (e) R.W. Hay, M.P. Pujari, Inorg. Chim. Acta 99 (1985) 75. (f) R. Menif, A.E. Martell, J. Chem. Soc. Chem. Commun. (1989) 1521. (g) K. Travis, D.H. Busch, J. Chem. Soc. Chem. Commun. (1970) 1041. (h) P.M. Schaber, J.C. Fettinger, M.R. Churchill, D. Nalewajek, K. Fries, Inorg. Chem. 27 (1988) 1641. (i) R.J. Motekaitis, A.E. Martell, J.-P. Lecomte, J.-M. Lehn, Inorg. Chem. 22 (1983) 609. (j) S.M. Nelson, Pure Appl. Chem. 52 (1980) 2461. (k) A. Lavery, S.M. Nelson, M.G.B. Drew, J. Chem. Soc. Dalton Trans. (1987) 2975. (l) M.G. Basallote, D. Chen, A.E. Martell, Inorg. Chem. 28 (1989) 3494. (m) L. Wei, A. Bell, K.H. Ahn, M.M. Holl, S. Warner, I.D. Williams, S.J. Lippard, Inorg. Chem. 29 (1990) 825.

[8] J.-M. Lehn, Pure Appl. Chem. 52 (1980) 2441.

[9] (a) M. Bourgoin, K.H. Wong, J.Y. Hui, J. Smid, J. Am. Chem. Soc. 97 (1975) 3462. (b) A. McAuley, S. Subramanian, T.W. Whitcombe, J. Chem. Soc. Chem. Commun. (1987) 539. (c) P.V. Bernhardt, P. Comba, L.R. Gahan, G.A. Lawrance, Aust. J. Chem. 43 (1990) 2035. (d) E.K. Barefield, D. Chueng, D.G. van Derveer, F. Wagner, J. Chem. Soc. Chem. Commun. (1981) 302. (e) L. Fabbrizzi, F. Forlini, A. Perotti, B. Seghi, Inorg.Chem. 23 (1984) 807. (f) L. Fabbrizzi, L. Montagna, A. Poggi, Th. A. Kaden, L.C. Siegfried, J. Chem. Soc. Dalton Trans. (1987) 2631. (g) E. Kimura, Y. Kuramoto, T. Koike, H. Fujioka, M. Kodama, J. Org. Chem. 55 (1990) 42. (h) L. Fabbrizzi, L. Montagna, A. Poggi, Th. A. Kaden, L.C. Siegfried, Inorg.Chem. 25 (1986) 2672.

[10] (a) I. Murase, K. Hamada, S. Ueno, S. Kida, Synth. React. Inorg. Met. Org. Chem. 13 (1983) 191. (b) M. Ciampolini, M. Micheloni, N. Nardi, F. Vizza, A. Buttafava, L. Fabbrizzi, A. Perotti, J. Chem. Soc. Chem. Commun. (1984) 998. (c) I. Murase, S. Ueno, S. Kida, Inorg. Chim. Acta 111 (1986) 57. (d) E.K. Barefield, K.A. Foster, G.M. Freeman, K.D. Hodges, Inorg. Chem. 25 (1986) 4663. (e) K. Wieghardt, I. Tolksdorf, W. Herrmann, Inorg. Chem. 24 (1985) 1230. (f) G.R. Weisman, D.J. Vachon, V.B. Johnson, D.A. Gronbeck, J. Chem. Soc. Chem. Commun. (1987) 886. (g) M. Ciampolini, L. Fabbrizzi, A. Perotti, A. Poggi, B. Seghi, F. Zanobini, Inorg. Chem. 26 (1987) 3527.

[11] A. Urfer, Th. A. Kaden, Helv. Chim. Acta 77 (1994) 23.
[12] S.S. Tandon, L.K. Thompson, J.N. Bridson, V. Mckee, A.J. Downard, Inorg. Chem. 31 (1992) 4635.
[13] L. Behle, M. Neuburger, M. Zehnder, Th. A. Kaden, Helv. Chim. Acta 78 (1995) 693.
[14] H. Weller, L. Siegfried, M. Neuburger, M. Zehnder, Th. A. Kaden, Helv. Chim. Acta 80 (1997) 2315.
[15] G.R. Weisman, D.J. Vachon, V.B. Johnson, D.A. Gronbeck, J. Chem. Soc. Chem. Commun. (1989) 2077.
[16] D. Hanke, K. Wieghard, B. Nuber, R.S. Lu, R.K. McMullen, T.F. Koetzle, R. Bau, Inorg. Chem. 32 (1993) 4300.
[17] B. Bleaney, K.D. Bowers, Proc. R. Soc. Lond. A. 214 (1952) 451.
[18] J.B. Flanagan, S. Margel, A.J. Bard, F.C. Anson, J. Am. Chem. Soc. 100 (1978) 4248.
[19] T. Kamiusuki, H. Okawa, E. Kitaura, M. Koikawa, N. Matsumoto, S. Kida, J. Chem. Soc. Dalton Trans. (1987) 2975.
[20] H. Weller, Th. A. Kaden, G. Hopfgartner, Polyhedron 17 (1998) 4543.
[21] H. Gampp, M. Maeder, Ch. Meyer, A.D. Zuberbühler, Talanta 32 (1985) 257.
[22] (a) G. Hopfgartner, C. Piguet, J.D. Henion, J. Am. Soc. Mass Spectrom. 5 (1994) 748. (b) C. Piguet, G, Bernardelli, G. Hopfgartner, Chem. Rev. 97 (1997) 2005.